[25] R. Sacco, D. Leuci, C. Tortorella, G. Fiore, F. Marinosci, and S. Antonaci, "Transforming growth factor β1 and soluble Fas serum levels in hepatocellular carcinoma," *Cytokine*, vol. 12, no. 6, pp. 811–814, 2000.

[26] X. P. Chen, H. Zhao, and X. P. Zhao, "Alternation of AFP-mRNA level detected in blood circulation during liver resection for HCC and its significance," *World Journal of Gastroenterology*, vol. 8, no. 5, pp. 818–821, 2002.

[27] X. Ding, L. Y. Yang, G. W. Huang et al., "Role of AFP mRNA expression in peripheral blood as a predictor for postsurgical recurrence of hepatocellular carcinoma: a systematic review and meta-analysis," *World Journal of Gastroenterology*, vol. 11, no. 17, pp. 2656–2661, 2005.

[28] N. Miura, Y. Maeda, T. Kanbe et al., "Serum human telomerase reverse transcriptase messenger RNA as a novel tumor marker for hepatocellular carcinoma," *Clinical Cancer Research*, vol. 11, no. 9, pp. 3205–3209, 2005.

[29] N. Miura, G. Shiota, T. Nakagawa et al., "Sensitive detection of human telomerase reverse transcriptase mRNA in the serum of patients with hepatocellular carcinoma," *Oncology*, vol. 64, no. 4, pp. 430–434, 2003.

[30] T. Hutchens and T. T. Yip, "New desorption strategies for the mass spectrometric analysis of macromolecules," *Rapid Communications in Mass Spectrometryvol*, vol. 7, pp. 576–580, 1993.

[31] F. Nomura, T. Tomonaga, K. Sogawa et al., "Identification of novel and downregulated biomarkers for alcoholism by surface enhanced laser desorption/ionization-mass spectrometry," *Proteomics*, vol. 4, no. 4, pp. 1187–1194, 2004.

[32] K. Sogawa, S. Itoga, T. Tomonaga, and F. Nomura, "Diagnostic values of surface-enhanced laser desorption/ionization technology for screening of habitual drinkers," *Alcoholism*, vol. 31, supplement s1, pp. S22–S26, 2007.

[33] V. Paradis, F. Degos, D. Dargère et al., "Identification of a new marker of hepatocellular carcinoma by serum protein profiling of patients with chronic liver diseases," *Hepatology*, vol. 41, no. 1, pp. 40–47, 2005.

[34] S. Kanmura, H. Uto, K. Kusumoto et al., "Early diagnostic potential for hepatocellular carcinoma using the SELDI ProteinChip system," *Hepatology*, vol. 45, no. 4, pp. 948–956, 2007.

[35] N. L. Anderson and N. G. Anderson, "The human plasma proteome: history, character, and diagnostic prospects," *Molecular & Cellular Proteomics*, vol. 1, no. 11, pp. 845–867, 2002.

[36] N. Hattori, S. Oda, T. Sadahiro et al., "YKL-40 identified by proteomic analysis as a biomarker of sepsis," *Shock*, vol. 32, no. 4, pp. 393–400, 2009.

[37] K. Sogawa, Y. Kodera, M. Satoh et al., "Increased serum levels of pigment epithelium-derived factor by excessive alcohol consumption-detection and identification by a three-step serum proteome analysis," *Alcoholism*, vol. 35, no. 2, pp. 211–217, 2011.

[38] M. Kadowaki, T. Sangai, T. Nagashima et al., "Identification of vitronectin as a novel serum marker for early breast cancer detection using a new proteomic approach," *Journal of Cancer Research and Clinical Oncology*, vol. 137, no. 7, pp. 1105–1115, 2011.

[39] M. Abulaizi, T. Tomonaga, M. Satoh et al., "The application of a three-step proteome analysis for identification of new biomarkers of pancreatic cancer," *International Journal of Proteomics*, vol. 2011, Article ID 628787, 13 pages, 2011.

[40] H. Umemura, M. Nezu, Y. Kodera et al., "Effects of the time intervals between venipuncture and serum preparation for serum peptidome analysis by matrix-assisted laser desorption/ionization time-of-flight mass spectrometry," *Clinica Chimica Acta*, vol. 406, no. 1-2, pp. 179–180, 2009.

[41] U. K. Laemmli, "Cleavage of structural proteins during the assembly of the head of bacteriophage T4," *Nature*, vol. 227, no. 5259, pp. 680–685, 1970.

[42] L. Anderson and J. Seilhamer, "A comparison of selected mRNA and protein abundances in human liver," *Electrophoresis*, vol. 18, no. 3-4, pp. 533–537, 1997.

[43] C. R. M. Y. Liang, C. K. Leow, J. C. H. Neo et al., "Proteome analysis of human hepatocellular carcinoma tissues by two-dimensional difference gel electrophoresis and mass spectrometry," *Proteomics*, vol. 5, no. 8, pp. 2258–2271, 2005.

[44] J. Kim, S. H. Kim, S. U. Lee et al., "Proteome analysis of human liver tumor tissue by two-dimensional gel electrophoresis and matrix assisted laser desorption/ionization-mass spectrometry for identification of disease-related proteins," *Electrophoresis*, vol. 23, no. 24, pp. 4142–4156, 2002.

[45] I. N. Lee, C. H. Chen, J. C. Sheu et al., "Identification of human hepatocellular carcinoma-related biomarkers by two-dimensional difference gel electrophoresis and mass spectrometry," *Journal of Proteome Research*, vol. 4, no. 6, pp. 2062–2069, 2005.

[46] O. L. Seung, S. J. Park, W. Kim et al., "Proteome analysis of hepatocellular carcinoma," *Biochemical and Biophysical Research Communications*, vol. 291, no. 4, pp. 1031–1037, 2002.

[47] J. T. Feng, Y. K. Liu, H. Y. Song et al., "Heat-shock protein 27: a potential biomarker for hepatocellular carcinoma identified by serum proteome analysis," *Proteomics*, vol. 5, no. 17, pp. 4581–4588, 2005.

[48] O. Blaschuk, K. Burdzy, and I. B. Fritz, "Purification and characterization of a cell-aggregating factor (clusterin), the major glycoprotein in ram rete testis fluid," *The Journal of Biological Chemistry*, vol. 258, no. 12, pp. 7714–7720, 1983.

[49] H. V. De Silva, W. D. Stuart, C. R. Duvic et al., "A 70-kDa apolipoprotein designated ApoJ is a marker for subclasses of human plasma high density lipoproteins," *The Journal of Biological Chemistry*, vol. 265, no. 22, pp. 13240–13247, 1990.

[50] I. P. Trougakos and E. S. Gonos, "Clusterin/Apolipoprotein J in human aging and cancer," *International Journal of Biochemistry and Cell Biology*, vol. 34, no. 11, pp. 1430–1448, 2002.

[51] T. L. Brown, B. C. Moulton, V. V. Baker, J. Mira, and J. A. K. Harmony, "Expression of apolipoprotein J in the uterus is associated with tissue remodeling," *Biology of Reproduction*, vol. 52, no. 5, pp. 1038–1049, 1995.

[52] C. Petropoulou, I. P. Trougakos, E. Kolettas, O. Toussaint, and E. S. Gonos, "Clusterin/apolipoprotein J is a novel biomarker of cellular senescence that does not affect the proliferative capacity of human diploid fibroblasts," *FEBS Letters*, vol. 509, no. 2, pp. 287–297, 2001.

[53] M. Redondo, E. Villar, J. Torres-Munoz, T. Tellez, M. Morell, and C. K. Petito, "Overexpression of clusterin in human breast carcinoma," *American Journal of Pathology*, vol. 157, no. 2, pp. 393–399, 2000.

[54] M. J. Xie, Y. Motoo, S. B. Su et al., "Expression of clusterin in human pancreatic cancer," *Pancreas*, vol. 25, no. 3, pp. 234–238, 2002.

[55] X. Chen, R. B. Halberg, W. M. Ehrhardt, J. Torrealba, and W. F. Dove, "Clusterin as a biomarker in murine and human intestinal neoplasia," *Proceedings of the National Academy of Sciences of the United States of America*, vol. 100, no. 16, pp. 9530–9535, 2003.

[56] Y. K. Kang, S. W. Hong, H. Lee, and W. H. Kim, "Overexpression of clusterin in human hepatocellular carcinoma," *Human Pathology*, vol. 35, no. 11, pp. 1340–1346, 2004.

ALCOHOLISM: CLINICAL AND EXPERIMENTAL RESEARCH

Vol. 37, No. S1
January 2013

Combined Proteomic Analysis of Liver Tissue and Serum in Chronically Alcohol-Fed Rats

Mako Yamada, Mamoru Satoh, Masanori Seimiya, Kazuyuki Sogawa, Sakae Itoga, Takeshi Tomonaga, and Fumio Nomura

Background: Proteomic approaches may provide new insights into pathological conditions associated with alcoholism. The aim of this study was to conduct a proteomic analysis of liver tissue and serum in chronically alcohol-fed rats using agarose 2-dimensional gel electrophoresis (2-DE) and 3-step serum proteome analysis.

Methods: A total of 12 rats were pair-fed nutritionally adequate liquid diet containing ethanol as 36% of the total energy or an isocaloric control diet for 2 months. Rat liver homogenates and cytosol fractions were subjected to agarose 2-DE. Serum samples were subjected to 3-step serum proteome analysis involving immunodepletion of abundant proteins followed by fractionation using reverse-phase high-performance liquid chromatography and 1-dimensional sodium dodecyl sulfate polyacrylamide gel electrophoresis (SDS-PAGE). Candidate proteins were digested with trypsin and identified using mass spectrometry. Observed differences in protein expression levels were confirmed using Western blotting.

Results: A total of 46 protein spots were found to be differentially expressed in the liver homogenates and cytosol fractions of alcohol-fed rats relative to pair-fed controls. The most notable change was down-regulation of a 29-kDa protein, which was subsequently identified as carbonic anhydrase III (CA III). Down-regulation of this protein in alcohol-fed rats was confirmed by Western blotting. The messenger RNA level of CA III was decreased as well. In rat serum, a total of 41 proteins were differentially expressed. Of these proteins, only betaine–homocysteine methyltransferase (BHMT) was also found to be differentially expressed in the liver.

Conclusions: A combined proteomic analysis of liver tissue and serum in chronically alcohol-fed rats revealed that the expression of CA III is significantly down-regulated in the liver of alcohol-fed rats. Our results also showed that BHMT expression is up-regulated in both the liver and serum of alcohol-fed rats.

Key Words: Lieber–DeCarli Liquid Diet, Proteomics, Alcoholic Liver Disease.

CHRONIC ALCOHOL CONSUMPTION causes liver damage through a variety of complex and incompletely understood mechanisms, including direct hepatotoxicity associated with ethanol (EtOH) metabolism, up-regulation of pro-inflammatory cytokines, and oxidative stress (Lieber, 2004). Proteomics is a promising tool for uncovering the mechanisms of alcohol-induced liver damage. Proteomics is the systematic large-scale identification and characterization of the proteome, which is defined as the complete set of proteins found in a given cell type in any particular state, and involves the measurement of protein expression and modifications using various techniques. Proteomic approaches have been used to identify new diagnostic markers and therapeutic targets in many fields of clinical medicine (Diamond et al., 2006; Smith et al., 2006). Proteomics is therefore likely to be a useful tool for gaining additional insights into those pathological conditions associated with alcoholism.

Currently, proteomic techniques can be broadly classified into 2 categories: gel-based and gel-free methods. Surface enhanced laser desorption/ionization time-of-flight mass spectrometry (SELDI-TOF MS) is an example of a sophisticated gel-free method (Weinberger et al., 2002). Previously, we used the SELDI technology to generate comparative protein profiles of consecutive serum samples obtained from alcoholic patients during abstinence and identified several novel biomarkers associated with the propensity for excessive alcohol consumption (Nomura et al., 2004; Sogawa et al., 2006). Although SELDI-TOF MS is suitable for detecting low-molecular-weight proteins, gel-based 2-dimensional electrophoresis (2-DE) is preferable for analyzing high-molecular-weight proteins. Conventional 2-DE, however, has some limitations in terms of sensitivity and reproducibility. Several methods have been developed to overcome these problems, one of which is the agarose 2-DE method, which has been shown to have higher loading capacity for first-

From the Department of Molecular Diagnosis (MY, MSe, SI, FN), Graduate School of Medicine, Chiba University, Chiba, Japan; Clinical Proteomics Research Center (MSa, KS, FN), Chiba University Hospital, Chiba, Japan; and Laboratory of Proteome Research (TT), National Institute of Biomedical Innovation, Osaka, Japan.

Received for publication December 20, 2011; accepted May 16, 2012.

Reprint requests: Fumio Nomura, MD, PhD, Department of Molecular Diagnosis and Division of Clinical Genetics and Proteomics, Graduate School of Medicine, Chiba University and Chiba University Hospital, 1-8-1 Inohana, Chuo-ku, Chiba City, Chiba 260-8670, Japan; Tel./Fax: +81-43-226-2324; E-mail: fnomura@faculty.chiba-u.jp

DOI: 10.1111/j.1530-0277.2012.01883.x

dimension isoelectric focusing (IEF) than 2-DE using immobilized pH gradient (IPG) gels (Oh-Ishi et al., 2000). This method not only allows for large-scale quantitative comparisons of protein expression, but is also capable of resolving proteins larger than 150 kDa, which are difficult to resolve using conventional 2-DE methods. We identified several novel proteins with altered expression in primary colorectal cancer cells using the agarose 2-DE approach (Tomonaga et al., 2004).

It is now feasible to conduct simultaneous proteomic analyses of tissues and serum from experimental animals. However, a technical challenge associated with serum proteomic analyses that must be overcome is the large dynamic range in the concentration of different proteins and peptides in serum, which may number in the thousands (Anderson and Anderson, 2002; Tirumalai et al., 2003). We recently described a simple and highly reproducible 3-step method (immunodepletion of abundant proteins followed by fractionation using reverse-phase high-performance liquid chromatography [HPLC] and 1-dimensional sodium dodecyl sulfate polyacrylamide gel electrophoresis [SDS-PAGE]) to identify potential disease marker candidates among low-abundance serum proteins (Kawashima et al., 2010). Using this method, we identified YKL-50 as a promising biomarker of sepsis (Hattori et al., 2009) and vitronectin as an indicator of the early stages of breast cancer (Kadowaki et al., 2011). In addition, using this 3-step serum proteomic analysis method, we found that the serum level of pigment epithelial-derived factor is elevated in excessive alcohol drinkers (Sogawa et al., 2011). In the present study, we used a combined proteomic approach to investigate changes in protein expression in both the liver and serum of rats chronically fed an alcohol-containing diet. We used the agarose 2-DE method to examine proteomic changes in rat liver homogenates and cytosol fractions and the 3-step method to evaluate proteomic changes in serum associated with chronic alcohol consumption.

MATERIALS AND METHODS

Sample Preparation

A total of 12 male Sprague–Dawley rats (Charles River Japan, Yokohama, Japan) weighing 140 to 150 g were used in this study. Rats were maintained at the laboratory animal facility of Chiba University Graduate School of Medicine, housed at 24 ± 1°C and under a 12-hour light/dark cycle. All animals were placed in the same room and caged individually. A total of 12 rats were pair-fed with a nutritionally adequate liquid diet containing EtOH as 36% of the total energy or an isocaloric control diet (Oriental Yeast Co., Tokyo, Japan) for 2 months as described by Lieber and Decarli (1989). Animal care was in accordance with our institutional guidelines. Subcellular fractionation of the liver was conducted as described previously (Nomura et al., 1983).

Two-Dimensional Gel Electrophoresis

Liver homogenates and cytosol samples were initially treated with lysis buffer (7 M urea, 2 M thiourea, 2% (w/v) CHAPS, 0.1 M dithiothreitol, 1% (w/v) Pharmalyte broad-range pH 3 to 10 ampholytes (GE Healthcare, Tokyo, Japan), and 0.16% Complete protease inhibitors (Roche Diagnostics, Mannheim, Germany). Agarose gels were used for first-dimension IEF (Oh-Ishi et al., 2000), and SDS-PAGE gels were used for the second-dimension separation (Laemmli, 1970). This method has a higher loading capacity than 2-DE methods using IPG gels for the IEF step. In addition, the agarose 2-DE method is capable of resolving proteins larger than 150 kDa, which are difficult to resolve using IPG gels (Oh-Ishi et al., 2000). The first-dimension agarose gels used in this study measured 260 × 3.4 mm o.d. and were cast in glass tubes. The second-dimension polyacrylamide gels were 6 to 12% T gradient or 12% T homogeneous slab gels and were 200 (width) × 120 (height) × 1.3 mm. The gradient gels were used for analyzing cytosol fractions, while the homogenous gels were used to analyze liver homogenate samples.

Samples (500 μg) were subjected to first-dimension IEF for 12,000 Vh at 4°C, followed by fixation in 10% trichloroacetic acid and 5% sulfosalicylic acid for 60 minutes at room temperature. After washing with deionized water for 60 minutes, the agarose gel was then transferred to a polyacrylamide gel. Following SDS-PAGE, the gel was fixed in a solution of 30% methanol and 10% acetic acid overnight, stained with Coomassie Brilliant Blue (CBB), then destained in 30% methanol containing 10% acetic acid.

Three-Step Serum Proteomic Analysis

Rat serum was separated by centrifugation at 1,500×g for 10 minutes at 4°C and then stored at −80°C until analysis. The samples were subjected to 3-step proteomic analysis as described previously (Sogawa et al., 2011). Briefly, the steps were as follows: (i) the most abundant proteins were removed through immunodepletion; (ii) proteins were fractionated using reverse-phase HPLC; and (iii) proteins were further separated using 1-dimensional SDS-PAGE. Finally, gels were silver stained and then destained in 30% methanol containing 10% acetic acid.

Protein Quantification Using 2-DE and SDS-PAGE Image Analysis

Agarose 2-DE and SDS-PAGE gels were processed using Scion Image analysis software (www.scioncorp.com) to determine the integrated densities of the sample protein spots and molecular weight marker protein spots (1 mg each) run on the same gel. The amount of protein contained in a stained spot was determined according to the ratio of the integrated density of the spot to the average density of the molecular weight marker protein spots (Satoh et al., 2005).

In-Gel Digestion of Proteins

Proteins separated by agarose 2-DE and SDS-PAGE were fragmented into peptides using a slight modification of a previously reported methodology for in-gel tryptic digestion (Satoh et al., 2005). CBB-stained protein spots in 2-DE gels were individually excised as squares of approximately 1 mm, destained in 50% (v/v) acetonitrile (ACN) containing 50 mM NH_4HCO_3 and then washed with deionized water. The gel pieces were dehydrated in 100% ACN for approximately 15 minutes and then dried using a TOMY CC-105 centrifugal concentrator (Tomy Digital Biology, Tokyo, Japan) for 60 minutes. Gel pieces were then immersed for 45 minutes at 4°C in 10 to 30 μl of 50 mM Tris buffer (pH 9.0) containing 50 ng/μl of trypsin (Roche Diagnostics). Excess trypsin was discarded and the gel pieces were stored for 24 hours at 37°C in a minimal volume (10 to 20 μl) of 50 mM Tris buffer (pH 9.0). Peptide fragments digested in the gel pieces diffused into the surrounding solution over 24 hours. The solution was then slowly transferred to 1.5-ml siliconized plastic test tubes and stored at 4°C. Peptide fragments remaining in the gel pieces were recovered after 20-minute incubations at room temperature in a minimal volume of 5% (v/v) formic acid containing 50% (v/v) ACN. The peptide-containing solutions were

pooled in siliconized tubes and stored at 4°C. The molar quantity of recovered peptide fragments was estimated from the staining intensity of the corresponding 2-DE gel spot.

Mass Spectrometry

A quantity of digested peptides roughly equivalent to 5 pmol of protein contained in a 2-DE spot was injected onto a 0.2 × 50 mm C18 column (AMR, Tokyo, Japan) attached to a MAGIC 2002 HPLC system (AMR). The flow rate of the mobile phase was maintained at 1 μl/min using a MAGIC variable splitter. The mobile-phase composition was programmed to change in 30-minute cycles with varying mixing ratios (r) of solvent A (2% (v/v) ACN and 0.1% (v/v) formic acid) to solvent B (90% (v/v) ACN and 0.1% (v/v) formic acid) as follows: linear gradient of r = 5 to 50% from t = 0 to 20 minutes, linear gradient of r = 50 to 85% from t = 20 to 21 minutes, constant r = 85% from t = 21 to 22 minutes, linear gradient of r = 85 to 5% from t = 22 to 23 minutes, and constant r = 5% from t = 23 to 30 minutes. Purified peptides were introduced from the HPLC column to a Q-star Pulsar i (Applied Biosystems, Foster City, CA) mass spectrometer. Both MS and MS/MS peptide spectra were collected in a data-dependent manner according to the manufacturer's operating specifications. The Mascot search engine (Matrix Science, London, UK) was used to identify proteins from the MS and MS/MS peptide spectra.

Western Blotting

Protein extracts were separated by SDS-PAGE on 10 to 20% gradient gels (XV PANTERA Gel; DRC, Tokyo, Japan). The proteins were transferred to polyvinylidene fluoride membranes (Millipore, Bedford, MA) in a tank-transfer apparatus (Bio-Rad, Hercules, CA), and the membranes were blocked with 0.5% skim milk in PBS. Antihuman carbonic anhydrase III (CA III) monoclonal antibody (R&D Systems, Minneapolis, MN) diluted 1:1,000, antimouse betaine–homocysteine methyltransferase (BHMT) polyclonal antibody diluted 1:2,000 and anti-β-actin diluted 1:500 in blocking buffer were used as primary antibodies. Horseradish peroxidase-conjugated rabbit antigoat IgG (Cappel, West Chester, PA) diluted 1:500 and polyclonal antimouse immunoglobulins/horseradish peroxidase (Dako Denmark A/S, Glostrup, Denmark) diluted 1:1,000 in blocking buffer were used as the secondary antibody. Antigens on the membrane were detected with enhanced chemiluminescence detection reagents (GE Healthcare UK Ltd., Buckinghamshire, UK), and NIH Image (Bethesda, MD) was used to measure the intensity of each spot. Bovine erythrocyte CA (Worthington Biochemical Corporation, Lakewood, NJ) was used as a positive control.

Real-Time PCR

Total RNA was extracted from the livers of alcohol-fed and control rats using an RNeasyTM Plus Mini kit (Qiagen, Tokyo, Japan). The cDNA was synthesized from total RNA using the First-Strand cDNA Synthesis kit for RT-PCR (AMV) (Roche Diagnostics). Using the cDNA as a template, CA III cDNA was amplified using the following primers: forward, 5′-GAAAGGCGAGTTCCAGATT-3′, reverse, 5′-TCAGTAGCAGCCACACAA-3′; fluorescein probe: 5′-TAATCACTTCGACCCATCGTGCCTGTTCC-fluorescein-3′; and LCRed640 probe: 5′-LCRed640-TGCTTGCCGGGACTATTGGACCTACCAT-phosphate-3′. Real-time quantitative PCR was performed using a Light Cycler Instrument (Roche Diagnostics).

Miscellaneous Methods

Total protein concentration was determined using the Bio-Rad Protein Assay kit with bovine serum albumin as the standard. Numerical data are presented as the mean ± SD. The statistical significance of differences was assessed using the Student's t-test; p-values <0.05 were considered significant.

RESULTS

Histological examination revealed significant fatty changes in the livers of alcohol-fed rats. This observation was in agreement with previous reports (Lieber and Decarli, 1989). Liver homogenates and the cytosol fractions obtained from 6 pairs of alcohol-fed and controls rats were separated using agarose 2-DE, and proteins were visualized by Coomassie blue staining. Representative electrophoretic patterns are shown in Figs 1 and 2.

Approximately 600 spots over the pH range of 3 to 10 and molecular weight range of 21.5 to 200 kDa were detected at the protein loadings used in this study. The staining intensity of 46 spots increased or decreased in samples from rats subjected to chronic alcohol consumption. Of these 46 spots, 8 spots were identified using LC-MS/MS (Table 1). The most striking difference in staining intensity between gels of alcohol-fed and control rat samples was observed with respect to Spot 1. The intensity of Spot 1 was markedly lower than that of the control in 2-DE gels of both liver homogenate and cytosol fraction samples from all 6 alcohol-fed rats (Figs 1 and 2). The protein contained in Spot 1 was identified as CA III using LC-MS/MS following in-gel trypsin digestion.

The differential expression of CA III was validated through immunoblotting. As indicated in Fig. 3, Western blotting analyses of liver homogenate and cytosol fraction samples using an antihuman CA III antibody showed a consistent and significant decrease in CA III expression in rats subjected to chronic alcohol consumption. Densitometric analysis of images of the immunoreactive protein band indicated that the level of CA III in the liver homogenate had decreased by 75% in alcohol-fed rats relative to control rats (C, 5.8 ± 6.8; A, 1.1 ± 0.8; p = 0.03). Likewise, the level of CA III in the cytosol fraction of alcohol-fed rats had decreased by 70% relative to the control rats (C, 1.9 ± 0.9; A, 0.5 ± 0.4; p = 0.003). Real-time PCR analysis indicated that the level of hepatic *CA III* mRNA was significantly lower in alcohol-fed rats than in their pair-fed controls. Using β-actin as a reference for normalization, real-time PCR showed that the level of *CA III* mRNA was 96% lower in the livers of alcohol-fed rats (Fig. 4).

Serum samples obtained from the 6 pairs of alcohol-fed and controls rats were subjected to the 3-step proteomic analysis to determine whether chronic alcohol consumption leads to alterations in the serum proteome. Representative electrophoretic patterns are shown in Fig. 5. The expression of 77 bands was found to be altered as a result of chronic alcohol consumption, and a total of 41 proteins were identified from these bands, as indicated in Table 2. Although CA III was not detected in the 3-step analysis, BHMT was found to be up-regulated (Fig. 5). Western blotting

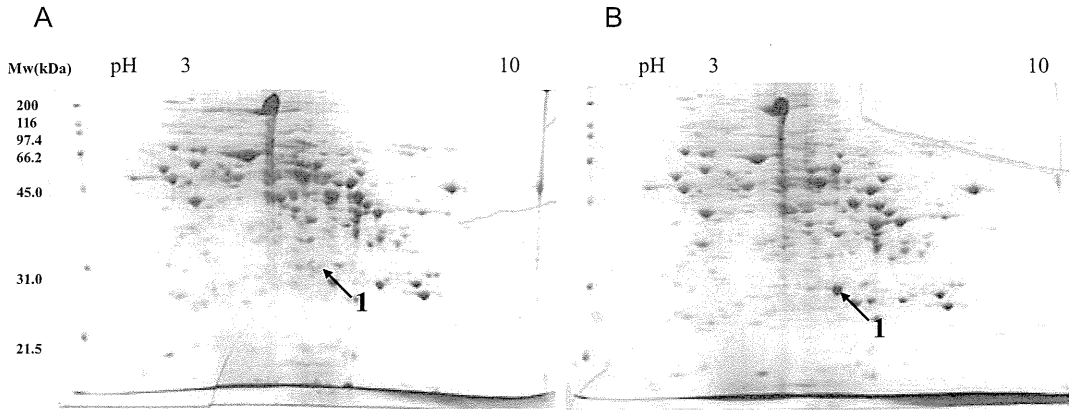

Fig. 1. Representative agarose 2-dimensional electrophoresis gels of liver homogenates obtained from alcohol-fed (**A**) and pair-fed control (**B**) rats. Spot 1 is significantly down-regulated in alcohol-fed rats.

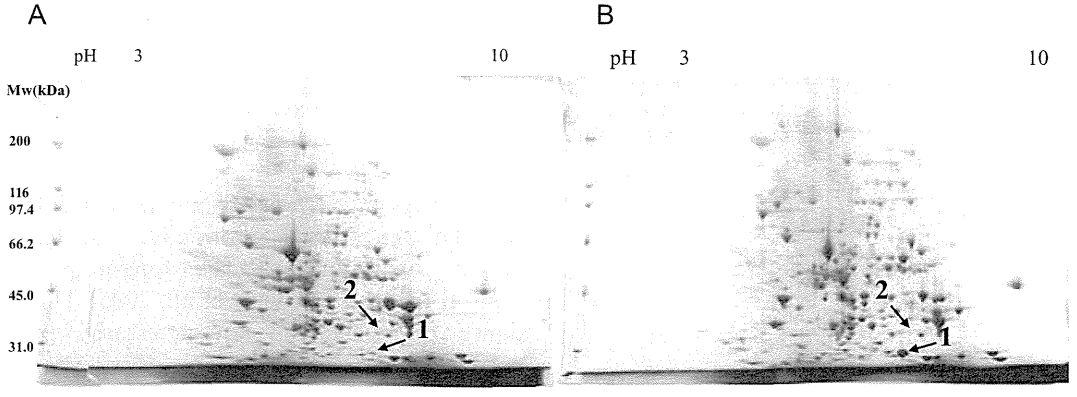

Fig. 2. Representative agarose 2-dimensional electrophoresis gels of liver cytosol obtained from alcohol-fed (**A**) and pair-fed control (**B**) rats. Spot 1 is significantly down-regulated in alcohol-fed rats, while Spot 2 is significantly up-regulated in alcohol-fed rats.

Table 1. Differentially Expressed Proteins in the Liver Homogenate and Cytosol Fraction of Alcohol-Fed Rats as Determined Using Agarose 2-DE and LC-MS/MS

No.	ID	Experimental mass (Da)	Theoretical mass (Da)	Score[a]	Queries matched[b]	Average volume ratio[c]	Gene ID
A. Up-regulated liver homogenate and cytosol fraction proteins in alcohol-fed rats							
1.	Cysteine sulfinic acid decarboxylase	50,000	55,214	547	11	2.4	60356
2.	Betaine–homocysteine *S*-methyltransferase	40,000	44,948	234	5	4.9	81508
3.	Argininosuccinate synthase	45,000	46,467	333	9	1.9	377549
4.	Glutathione *S*-transferase alpha5	25,000	25,200	265	7	2.6	494500
5.	ATP synthase alpha chain, mitochondrial precursor	45,000	58,790	314	8	2.9	65262
6.	Sulfotransferase family cytosolic IB member 1	40,000	34,813	113	2	4.9	64305
7.	Alcohol dehydrogenase	40,000	36,352	50	1	4.9	6220527
8.	T-complex protein 1, alpha subunit	45,000	60,322	46	1	2.9	24818
9.	GI/S-specific cyclin D2	45,000	32,805	29	1	2.9	64033
B. Down-regulated liver homogenate and cytosol fraction proteins in alcohol-fed rats							
1.	Carbonic anhydrase III	29,000	29,282	366	11	−4.7	54232
2.	Glutathione *S*-transferase Mu1	25,000	25,766	123	3	−1.9	24424

[a]MOWSE score of candidate proteins.
[b]Number of peptide fragments yielding informative MS/MS.
[c]A positive value signifies up-regulation and a negative value signifies down-regulation in terms of fold-differences.

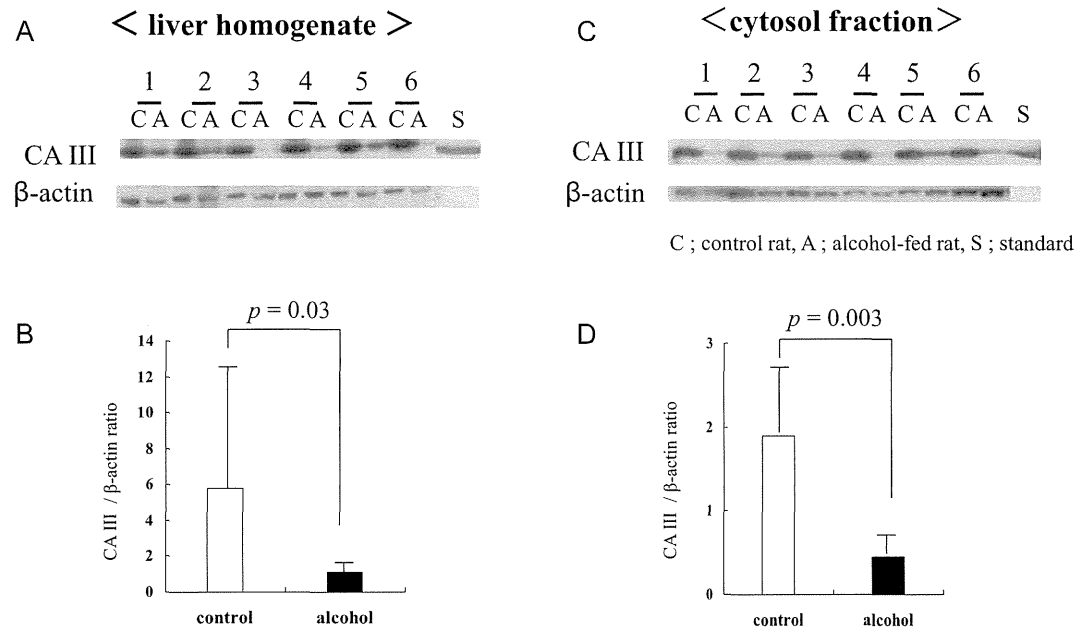

Fig. 3. Western blotting analysis of hepatic carbonic anhydrase III (CA III) in rat liver homogenate (**A**) and the cytosol fraction (**C**). The intensity of each band was determined using NIH Image analysis and the relative mean. CA III between alcohol-fed and control rats normalized to that of β-actin were calculated. The CA III levels in alcohol-fed and control rats were: 1.1 ± 0.8 and 5.8 ± 6.8, respectively, in the homogenates (**B**) and 0.5 ± 0.4 and 1.9 ± 0.9, respectively, in the cytosol fraction (**D**). The differences were statistically significant.

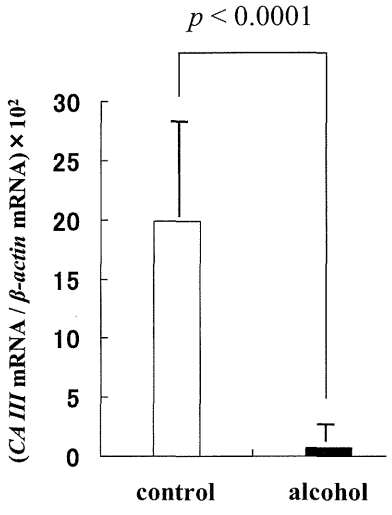

Fig. 4. Comparison of the hepatic carbonic anhydrase III mRNA level in alcohol-fed and control rats as determined using real-time quantitative PCR. In this experiment, β-actin was used as a reference for normalization of quantitative determinations (C: 0.199 ± 0.106, A: 0.007 ± 0.013). The difference was statistically significant.

confirmed the increase in expression of BHMT both in the liver and serum of alcohol-fed rats (Fig. 6).

DISCUSSION

The complete sequencing of the human genome has opened the door for comprehensive analyses of the transcriptome and proteome. Transcriptome analyses utilizing DNA microarrays have revealed unique patterns of gene expression that are clinically informative. This technique has been applied to study the effects of long-term alcohol consumption on the liver (Deaciuc et al., 2005). However, the abundance of mRNA is not necessarily predictive of the corresponding expression level of a given protein, as data regarding comprehensive protein expression (the proteome) are most relevant to characterizing a biological system. Furthermore, DNA microarrays have limited utility for the analysis of clinical specimens, such as serum or urine for the purpose of uncovering biomarkers of clinical significance. As a result, there is growing interest in the use of proteomic technologies for comprehensive identification of disease-specific alterations in protein expression. The great advantage of proteomic analyses is that proteins identified using these techniques are often good diagnostic and/or therapeutic marker candidates. Obtaining information at the level of the proteome is also necessary to unravel the critical changes involved in disease pathogenesis. Using 2-DE, Wirth and Vesterberg (1988) reported changes in the expression of liver cytosolic proteins after EtOH exposure in rats. They found pronounced differences in the relative abundance of several protein spots in EtOH-exposed rats as compared with controls. However, the identity of most of the proteins involved was not determined.

Long-term alcohol consumption causes liver damage through a complex process involving hepatotoxicity linked to EtOH metabolism, up-regulation of proinflammatory cytokines, and oxidative stress (Lieber, 2004). Mitochondria are particularly susceptible to increased formation of reactive oxygen species. Venkatraman and colleagues (2004) used a

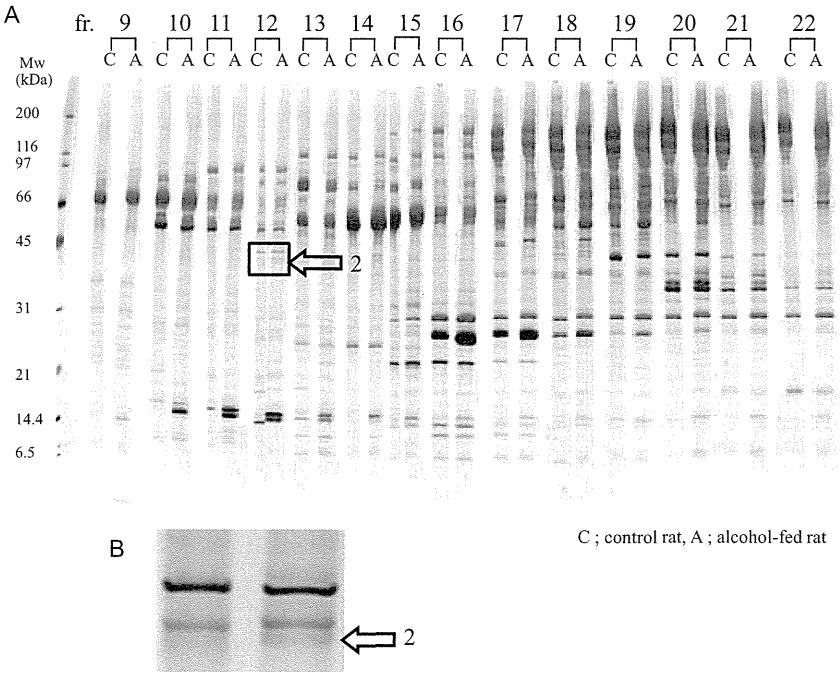

Fig. 5. (**A**) Results of 3-step proteomic analysis of serum obtained from alcohol-fed and pair-fed control rats. The gels were stained with silver. A total of 77 differentially expressed bands were detected in the serum of alcohol-fed rats, from which 41 proteins were identified. (**B**) Enlarged view of the region marked by the square in (**A**). Arrow in (**A**) and (**B**) indicates protein up-regulated in the serum of alcohol-fed rats, identified as betaine–homocysteine methyltransferase.

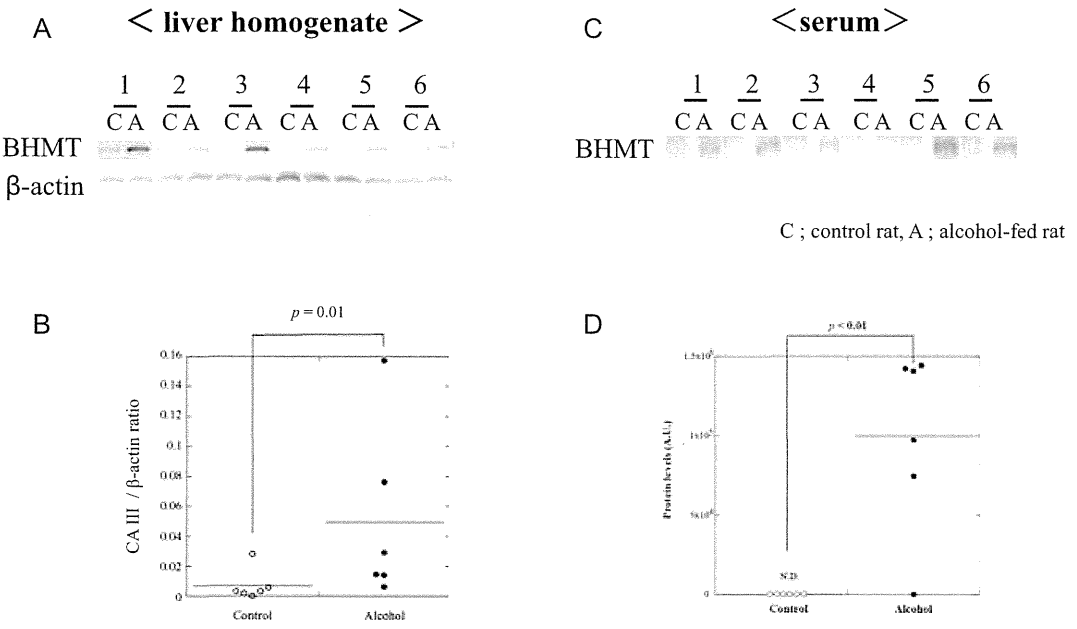

Fig. 6. Western blotting analysis of hepatic betaine–homocysteine methyltransferase (BHMT) in rat liver homogenates (**A**) and serum (**C**). The volume of each band was determined using image analysis software. The relative mean BHMT in the liver homogenates of alcohol-fed and control rats was calculated and normalized to that of β-actin. The volume of the BHMT band was significantly greater in samples from the alcohol-fed rats ($p = 0.01$) (**B**). Similarly, the volume of the BHMT band was significantly greater in the serum of alcohol-fed rats ($p < 0.01$) (**D**).

conventional 2-DE and blue native gel electrophoresis proteomic analysis to evaluate changes in the levels of mitochondrial proteins following chronic voluntary alcohol consumption in rats. Their study revealed that the expression of 45 proteins significantly changes as a consequence of chronic alcohol consumption. Of these 45 proteins, 25 had not been previously linked to adverse effects associated with alcohol consumption.

Table 2. Differentially Expressed Proteins in the Serum of Alcohol-Fed Rats as Determined Using the 3-Step Method

No.	ID	Experimental mass (Da)	Theoretical mass (Da)	Score[a]	Queries matched[b]	Average volume ratio[c]	Fraction No.	Gene ID
A. *Up-regulated rat serum proteins in alcohol-fed rats*								
1.	alpha-1-inhibitor III precursor	25,000	19,345	156	3	1.7	9	497794
2.	betaine–homocysteine methyltransferase	45,000	48,828	203	5	1.5	13	81508
3.	alpha-2-glycoprotein 1, zinc	40,000	33,996	251	5	1.7	14	25294
4.	apolipoprotein E	32,000	35,847	648	13	2.0	21	25728
5.	alpha-1-macroglobulin precursor	32,000	167,019	338	6	2.0	21	252922
6.	ceruloplasmin	32,000	120,764	88	2	1.4	10	24268
7.	clusterin precursor	40,000	51,342	256	5	1.4	15	24854
8.	complement C3 precursor	21,000	186,342	296	6	2.0	21	24232
9.	complement factor B	60,000	123,960	271	5	2.2	11	294257
10.	complement component 3	50,000	186,206	891	18	3.4	20	24232
11.	contrapsin-like protease inhibitor	21,000	45,653	174	3	1.6	13	24794
12.	corticosteroid binding globulin precursor	50,000	44,643	137	3	3.4	20	299270
13.	C-reactive protein, pentraxin-related	29,000	25,452	104	2	1.4	15	25419
14.	fetuin beta	50,000	41,506	419	10	2.2	11	83928
15.	hemoglobin alpha 2 chain	15,000	15,275	289	5	3.9	11	360504
16.	inter-alpha-inhibitor H4 heavy chain	30,000	103,543	260	4	1.4	15	54404
17.	inter-alpha trypsin inhibitor, heavy chain 3	40,000	99,036	123	2	1.7	14	50693
18.	inter-alpha trypsin inhibitor H4 heavy chain	32,000	103,543	209	4	1.4	17	54404
19.	murinoglobulin 1 homolog	31,000	165,221	171	6	1.7	9	497794
20.	preproapolipoprotein A-I	29,000	30,069	615	17	1.6	13	25081
21.	proteosome subunit, beta type 9	25,000	23,310	104	2	1.4	17	24967
22.	serine protease inhibitor 1	40,000	36,760	176	3	1.7	14	299282
23.	serine protease inhibitor A3N precursor	50,000	46,622	574	11	3.4	20	24795
24.	serum amyloid A4	14,000	15,982	259	5	6.2	12	365245
25.	serum amyloid P-component	31,000	26,159	325	8	1.4	11	29339
26.	transthyretin precursor (Prealbumin)	14,000	15,710	397	6	1.6	10	24856
27.	vitamin D-binding protein precursor	50,000	53,482	248	6	2.2	11	24384
28.	vitronectin	17,000	54,644	107	3	4.2	16	29169
B. Down-regulated rat serum proteins in alcohol-fed rats								
1.	aldolase A	45,000	39,235	227	4	−1.4	12	24189
2.	alpha-1-macroglobulin precursor	50,000	167,053	218	5	−3.6	17	252922
3.	alpha-2u globulin precursor	20,000	20,169	186	4	−1.7	10	259246
4.	apolipoprotein A IV precursor	40,000	44,429	845	19	−1.6	21	25080
5.	apolipoprotein C-IV	20,000	14,522	64	2	−1.5	11	680551
6.	complement C3 precursor	50,000	186,342	300	7	−3.6	17	24232
7.	complement C4 precursor	50,000	192,042	177	4	−3.6	17	24233
8.	creatine kinase	43,000	42,992	389	9	−1.4	12	24265
9.	gelsolin	80,000	86,014	325	6	−1.4	16	296654
10.	histidine-rich glycoprotein	80,000	57,545	61	1	−1.4	16	17016
11.	inter-alpha trypsin inhibitor, heavy chain 3	80,000	99,036	176	4	−1.4	16	50693
12.	orosomucoid 1 (Alpha-1-acid glycoprotein)	45,000	23,560	137	3	−1.4	12	24614
13.	plasma kallikrein precursor	45,000	71,227	103	3	−3.6	17	25048
14.	retinol binding protein 4, plasma	25,000	23,205	170	4	−1.4	8	25703
15.	serine protease inhibitor A3K precursor	45,000	45,653	146	3	−1.4	12	24794
16.	serine protease inhibitor A3L precursor	45,000	45,248	150	3	−1.4	12	299282
17.	transthyretin precursor (Prealbumin)	17,000	15,710	119	2	−3.4	12	24856

[a]MOWSE score of candidate proteins.
[b]Number of peptide fragments yielding informative MS/MS.
[c]A positive value signifies up-regulation and a negative value signifies down-regulation in terms of fold-differences.

More recently, Klouchkova and colleagues (2006) conducted a 2-DE-based proteomic analysis to examine changes in protein expression in the liver of rats inbred to consume high levels of alcohol. A total of 118 spots were found to be significantly differentially expressed in the alcohol-consuming rats; the majority of these proteins were enzymes involved in glycolysis, gluconeogenesis, fatty acid oxidation, protein synthesis, and antioxidant activity.

These disease proteomics studies primarily relied on a combination of 2-DE for separation and visualization of proteins and MS for protein identification. The development of IPG gels has led to great improvement in terms of reproducibility; however, the protein loading capacity of IPG gels is such that it permits display only of relatively abundant proteins. Oh-Ishi and colleagues (2000) demonstrated that agarose 2-DE has a higher protein loading capacity than does conventional 2-DE utilizing IPG gels for IEF. In this study, we took advantage of the agarose 2-DE method to examine liver tissues obtained from rats subjected to long-term alcohol consumption using the Lieber–DeCarli liquid

diet. We found a total of 46 spots that were either up-regulated or down-regulated in expression based upon intensity in gels of liver tissues from alcohol-consuming rats. We initially focused on a 29-kDa protein markedly down-regulated in the liver of alcohol-fed rats that was subsequently identified as CA III.

Carbonic anhydrases are widespread zinc-containing enzymes, with at least 14 different isoforms present in mammals. Some CA isozymes are cytosolic (including CA I, CA II, CA III, and CA VII), while others are membrane-bound (including CA IV, CA IX, CA XII, and CA XIV). The CA III enzyme plays important roles in several cellular processes; it is present in the cytosol of rat liver cells and is unique among the CAs in that it also possesses phosphatase activity. The primary function of CAs, including CA III, is to catalyze the interconversion of CO_2 and HCO_3^- to maintain the acid–base balance in tissues. CA III has 2 sulfhydryl groups, and thus it has been suggested that the enzyme plays a role in scavenging oxygen radicals in cells. Cabiscol and Levine (1995) reported that CA III is very sensitive to oxidative modification, while Elchuri and colleagues (2005) reported that CA III expression is down-regulated in CuZn superoxide dismutase-deficient mice. Interestingly, CA III also reportedly acts as an antioxidant, preventing H_2O_2-induced apoptosis (Ishii et al., 2005). Henkel and colleagues (2006) reported that CA III is down-regulated in CCl_4-induced hepatic fibrosis in mice. The mechanism of CCl_4-induced liver injury is complex and incompletely understood, but is known to involve formation of highly reactive radicals that lead to lipid peroxidation. As oxidative stress is also involved in alcoholic liver injury, it is likely that the down-regulation of CA III observed in this study reflects the effect of long-term alcohol exposure in the liver. In an earlier study, Parkkila and colleagues (1999) showed that the level of CA III in the liver is enhanced after EtOH consumption in uncastrated micropigs, indicating interspecies differences with respect to how long-term alcohol consumption affects hepatic CA III expression. It remains to be investigated how the down-regulation of hepatic CA III expression observed in rats in this study relates to alcohol-induced liver injury in humans.

In searching for biomarkers of alcoholic liver diseases, Zhao and colleagues (2011) reported that it is preferable to conduct proteomic analyses of liver tissue and serum simultaneously. Increased expression of a particular protein in the liver does not necessarily mean that the serum concentration of that protein would also be elevated. Indeed, we found that the level of only 1 protein, BHMT, was higher than the control in both the liver and serum of alcohol-fed rats. Proteomic technology is advancing rapidly, and we expect that a number of other proteins will be shown to behave in a similar way. Newton and colleagues (2009) reported that BHMT is associated with alcoholic fatty liver, and several investigators have detected BHMT in proteomic studies involving the liver (Liang et al., 2005; Øverbye et al., 2007). In addition, Shinohara and colleagues (2010) showed that BHMT is up-regulated in the liver of alcohol-fed rats. The present study is the first report demonstrating that BHMT is up-regulated both in the liver and in the serum as a result of chronic alcohol consumption. The diagnostic relevance of this finding with respect to alcoholism remains to be determined. It is also unclear what level of alcohol consumption results in up-regulation of BHMT in humans. It is noteworthy that hepatic BHMT in rats fed with alcohol-containing diet for 3 weeks instead of 8 weeks was not up-regulated (data not shown).

A number of proteins other than CA III and BHMT were found to be altered as a result of chronic alcohol consumption in rats. In-depth analyses of how these proteins are involved in alcohol-induced liver injury pathways are thus needed. Moreover, the biological relevance of some of the changes in protein expression we observed remains to be clarified. Since proteins functioning as antioxidants are included in the list, we are planning to conduct a proteomic analysis that can selectively evaluate oxidized proteins in the liver (Sawada et al., 2008).

REFERENCES

Anderson NL, Anderson NG (2002) The human plasma proteome: history, character, and diagnostic prospects. Mol Cell Proteomics 1:845–867.

Cabiscol E, Levine RL (1995) Oxidative modification of carbonic anhydrase III. J Biol Chem 270:14742–14747.

Deaciuc IV, Song Z, McClain CJ (2005) Lessons from large-scale gene profiling of the liver in alcoholic liver disease. Hepatol Res 31:187–192.

Diamond DL, Proll SC, Jacobs JM, Chan EY, Camp DG II, Smith RD, Katze MG (2006) HepatoProteomics: applying proteomic technologies to the study of liver function and disease. Hepatology 44:299–308.

Elchuri S, Oberley TD, Qi W, Eisenstein RS, Roberts J, Remmen HV, Epstein CJ, Huang TT (2005) CuZnSOD deficiency leads to persistent and widespread oxidative damage and hepatocarcinogenesis later in life. Oncogene 24:367–380.

Hattori N, Oda S, Sadahiro T, Nakamura M, Abe R, Shinozaki K, Nomura F, Tomonaga T, Matsusita K, Kodera Y, Sogawa K, Satoh M, Hirasawa H (2009) YKL-40 identified by proteomic analysis as a biomarker of sepsis. Shock 32:393–400.

Henkel C, Roderfeld M, Weiskirchen R, Berres ML, Hillebrandt S, Lammert F, Meyer HE, Stühler K, Graf J, Roeb E (2006) Changes of the hepatic proteome in murine models for toxically induced fibrogenesis and sclerosing cholangitis. Proteomics 6:6538–6548.

Ishii Y, Akazawa D, Aoki Y, Yamada H, Oguri K (2005) Suppression of carbonic anhydrase III mRNA level by an aryl hydrocarbon receptor ligand in primary cultured hepatocytes of rat. Biol Pharm Bull 28:1087–1090.

Kadowaki M, Sangai T, Nagashima T, Sakakibara M, Yoshitomi H, Takano S, Sogawa K, Umemura H, Fushimi K, Nakatani Y, Nomura F, Miyazaki M (2011) Identification of vitronectin as a novel serum marker for early breast cancer detection using a new proteomic approach. J Cancer Res Clin Oncol 137:1105–1115.

Kawashima Y, Fukutomi T, Tomonaga T, Takahashi H, Nomura F, Maeda T, Kodera Y (2010) High-yield peptide-extraction method for the discovery of subnanomolar biomarkers from small serum samples. J Proteome Res 9:1694–1705.

Klouchkova I, Hrncirova P, Mechref Y, Arnold RJ, Li TK, McBride WJ, Novotny MV (2006) Changes in liver protein abundance in inbred alcohol preferring rats due to chronic alcohol exposure, as measured through a proteomics approach. Proteomics 6:3060–3074.

Laemmli UK (1970) Cleavage of structural proteins during the assembly of the head of bacteriophage. Nature 227:680–685.

Liang CR, Leow CK, Neo JC, Tan GS, Lo SL, Lim JW, Seow TK, Lai PB, Chung MC (2005) Proteome analysis of human hepatocellular carcinoma

tissues by two-dimensional difference gel electrophoresis and mass spectrometry. Proteomics 5:2258–2271.

Lieber CS (2004) Alcoholic fatty liver: its pathogenesis and mechanism of progression to inflammation and fibrosis. Alcohol 34:9–19.

Lieber CS, Decarli LM (1989) Liquid diet technique of ethanol administration. Alcohol Alcohol 24:197–211.

Newton BW, Russell WK, Russell DH, Ramaiah SK, Jayaraman A (2009) Liver proteome analysis in a rodent model of alcoholic steatosis. J Proteome Res 8:1663–1671.

Nomura F, Pikkarainen PH, Jauhonen P, Arai M, Gordon ER, Baraona E, Lieber CS (1983) Effect of ethanol administration on the metabolism of ethanol in baboons. J Pharmacol Exp Ther 227:78–83.

Nomura F, Tomonaga T, Sogawa K, Ohashi T, Nezu M, Sunaga M, Kondo N, Iyo M, Shimada H, Ochiai T (2004) Identification of novel and down-regulated biomarkers for alcoholism by surface enhanced laser desorption/ionization-mass spectrometry. Proteomics 4:1187–1194.

Oh-Ishi M, Satoh M, Maeda T (2000) Preparative two-dimensional gel electrophoresis with agarose gels in the first dimension for high molecular mass proteins. Electrophoresis 21:1653–1669.

Øverbye A, Fengsrud M, Seglen PO (2007) Proteomic analysis of membrane-associated proteins from rat liver autophagosomes. Autophagy 3:300–322.

Parkkila S, Halsted CH, Villanueva JA, Väänänen HK, Niemelä O (1999) Expression of testosterone-dependent enzyme, carbonic anhydrase III and oxidative stress in experimental alcoholic liver disease. Dig Dis Sci 44: 2205–2213.

Satoh M, Haruta-Satoh E, Omori A, Oh-Ishi M, Kodera Y, Furudate S, Maeda T (2005) Effect of thyroxine on abnormal pancreatic proteomes of the hypothyroid rdw rat. Proteomics 5:1113–1124.

Sawada A, Ueno T, Kawashima Y, Haruta-Satoh E, Oh-Ishi M, Kodera Y, Maeda T (2008) Protein carbonyl detection by two-dimensional fluorescence difference gel electrophoresis. J Electrophor 52:9–17.

Shinohara M, Ji C, Kaplowitz N (2010) Differences in betaine-homocysteine methyltransferase expression, endoplasmic reticulum stress response, and liver injury between alcohol-fed mice and rats. Hepatology 51:796–805.

Smith L, Lind MJ, Welham KJ, Camkwell L (2006) Cancer proteomics and its application to discovery and therapy response markers in human cancer. Cancer 107:232–241.

Sogawa K, Itoga S, Tomonaga T, Nomura F (2006) Diagnostic values of surface-enhanced laser desorption/ionization technology for screening of habitual drinkers. Alcohol Clin Exp Res 31:S22–S26.

Sogawa K, Kodera Y, Satoh M, Kawashima Y, Umemura H, Maruyama K, Takizawa H, Yokosuka O, Nomura F (2011) Increased serum levels of pigment epithelium-derived factor by excessive alcohol consumption-detection and identification by a three-step serum proteome analysis. Alcohol Clin Exp Res 35:211–217.

Tirumalai RS, Chan KC, Prieto DA, Issaq HJ, Conrads TP, Veenstra TD (2003) Characterization of the low molecular weight human serum proteome. Mol Cell Proteomics 2:1096–1103.

Tomonaga T, Matsushita K, Yamaguchi S, Oh-Ishi M, Kodera Y, Maeda T, Shiamda H, Ochiai T, Nomura F (2004) Identification of altered protein expression and post-translational modifications in primary colorectal cancer by using agarose two-dimensional gel electrophoresis. Clin Cancer Res 10:2007–2014.

Venkatraman A, Landar A, Davis AJ, Chamlee L, Sanderson T, Kim H, Page M, Pompilius M, Ballinver S, Darley-Usamar V, Bailey SM (2004) Modification of the mitochondrial proteome in response to the stress of ethanol-dependent hepatotoxicity. J Biol Chem 279:22092–22101.

Weinberger SR, Dalmasso SR, Fung ET (2002) Current achievements using Protein Chip Array technology. Curr Opin Chem Biol 6:86–91.

Wirth PJ, Vesterberg O (1988) Rat liver cytosolic protein changes after ethanol exposure studied by two-dimensional electrophoresis. Electrophoresis 9:47–53.

Zhao Z, Yu M, Crabb D, Xu Y, Liangpunsakul S (2011) Ethanol-induced alterations in fatty acid-related lipids in serum and tissues in mice. Alcohol Clin Exp Res 35:229–234.

MCP Papers in Press. Published on January 28, 2013 as Manuscript M112.024802

Integrated proteomics identified novel activation of dynein IC2-GR-COX-1 signaling in NF1 disease model cells

Mio Hirayama[1]*, Daiki Kobayashi[1]*, Souhei Mizuguchi[1], Takashi Morikawa[1], Megumi Nagayama[1], Uichi Midorikawa[1], Masayo M. Wilson[1], Akiko N. Nambu[1], Akiyasu C. Yoshizawa[2], Shin Kawano[3], and Norie Araki[1**]

[1]Department of Tumor Genetics and Biology, Graduate school of Medical Sciences, Kumamoto University, 1-1-1, Honjo, Chuo-ku, Kumamoto 860-8556, Japan.

[2]Bioinformatics Center, Institute for Chemical Research, Kyoto University, Gokasho, Uji, Kyoto 611-0011, Japan

[3]Database Center for Life Science, Research Organization of Information and Systems, 2-11-16, Yayoi, Bunkyo-ku, Tokyo 113-0032, Japan

*These authors contributed equally to this work.

**To whom correspondence should be addressed: Norie Araki, Ph. D.

Department of Tumor Genetics and Biology, Graduate school of Medical Sciences,

Kumamoto University, 1-1-1, Honjo, Kumamoto 860-8556, Japan

Tel; +81-96-373-5119, Fax; +81-96-373-5210

E-mail; nori@gpo.kumamoto-u.ac.jp

Running Title: Integrated proteomics of NF1 disease model cells

Abbreviations

NF1-KD, NF1 knockdown; 2D-DIGE, two-dimensional fluorescence difference gel electrophoresis; iTRAQ, isobaric tagging for relative and absolute quantitation; iPEACH, Integrated Protein Expression Analysis Chart; NGF, nerve growth factor; GO, gene ontology; MANGO, Molecular Annotation by Gene Ontology; Qq-TOF, quadrupole/quadrupole/time-of-flight mass spectrometers; dynein IC, dynein intermediate chain; GR, glucocorticoid receptor; COX-1, cyclooxygenase-1; siRNA, short interfering RNA; MPNST, malignant peripheral nerve sheath tumor; PGE2, prostaglandin E2

Foot note

Authors' present addresses;

S Mizuguchi, Dept. Neurosurgery, Faculty of Medicine, University of Miyazaki, 5200 Kihara Kiyotake Miyazaki , 889-1692, Japan

T Morikawa, Mitsubishi Chemical Medience Corporation, 14, Sunayama, Kamisu, Ibaraki 314-0255, Japan.

U. Midorikawa, Healthcare Systems Laboratories, Sharp Corp. 1-9-2, Nakase, Mihama-ku, Chiba, 261-8520, JapanA. C. Yoshizawa, Koichi Tanaka Laboratory of Advanced Science and Technology, Shimadzu Corporation, Nishinokyo-Kuwabara-cho, Nakagyo-ku, Kyoto 604-8511, Japan

Summary

Neurofibromatosis type 1 (NF1) tumor suppressor gene product, neurofibromin, functions in part as a Ras-GAP, and though its loss is implicated in the neuronal abnormality of NF1 patients, its precise cellular function remains unclear. To study the molecular mechanism of NF1 pathogenesis, we prepared NF1 gene knockdown (KD) PC12 cells, as a NF1 disease model, and analyzed their molecular (gene and protein) expression profiles with a unique integrated proteomics approach, comprising iTRAQ, 2D-DIGE, and DNA microarrays, using an integrated protein/gene expression analysis chart (iPEACH). In NF1-KD PC12 cells showing abnormal neuronal differentiation after NGF treatment, of 3198 molecules quantitatively identified and listed in iPEACH, 97 molecules continuously up- or down-regulated over time were extracted. Pathway/network analysis further revealed overrepresentation of calcium signaling and transcriptional regulation by glucocorticoid receptor (GR) in the upregulated protein set, while nerve system development was overrepresented in the downregulated protein set. The novel upregulated network we discovered, "dynein IC2-GR-COX-1 signaling," was then examined in NF1-KD cells. Validation studies confirmed that NF1 knockdown induces altered splicing and phosphorylation patterns of dynein IC2 isomers, upregulation and accumulation of nuclear GR, and increased COX-1 expression in NGF-treated cells. Moreover, the neurite retraction phenotype observed in NF1-KD cells was significantly recovered by knockdown of the dynein IC2-C isoform and COX-1. In addition, dynein IC2 siRNA significantly inhibited nuclear translocation/accumulation of GR and upregulation of COX-1 expression. These results suggest that dynein IC2 upregulates GR nuclear translocation/accumulation, and subsequently causes increased COX-1 expression, in this NF1 disease model. Our integrated proteomics strategy, which combines multiple approaches, demonstrates that NF1-related neural abnormalities are, in part, caused by upregulation of dynein IC2-GR-COX-1

signaling, which may be a novel therapeutic target for NF1.

Introduction

Neurofibromatosis type 1 (NF1) is an autosomal dominantly inherited disorder with an estimated prevalence of 1 in 3,000 people (1). The hallmarks of NF1 include development of benign tumors of the peripheral nervous system and increased risk of malignancies. The phenotype of NF1 is highly variable, with several organ systems affected including the skin, bones, irises, and central and peripheral nervous systems. The effects on the nervous system are manifested in multiple neurofibroma, gliomas, and learning disabilities.

The NF1 gene is located on chromosome 17q11.2 and encodes a large protein of 2,818 amino acids, neurofibromin (2). Because the great majority of NF1 gene mutations frequently found in NF1 patients disturb the expression of intact neurofibromin, functional disruption of neurofibromin is potentially relevant to the expression of some or all of the abnormalities that occur in NF1 patients (3). A region centered around 360 amino acid residues encoded by the NF1 gene shows significant homology to the known catalytic domains of mammalian Ras GTPase-activating protein (p120 GAP). This region is also similar to yeast IRA1/2 proteins, which have been shown to interact with Ras and mediate hydrolysis of Ras-bound GTP to GDP, resulting in inactivation of Ras protein function. The GAP-related domain of the NF1 gene product also stimulates Ras GTPase and consequently inactivates Ras protein (4-6). In our previous report, we demonstrated a novel role of neurofibromin in neuronal differentiation in conjunction with regulation of Ras activity via its GAP-related domain using nerve growth factor (NGF)-stimulated PC12 cells as a model for neuronal cells (6). We also found that a novel neurofibromin interacting protein CRMP-2, identified with the screening of binding proteins of neurofibromin C-terminal domain by iTRAQ, upregulates the phosphorylation patterns in the NF1 siRNA treated PC12 cells compared with those of control cells through two-dimensional (2D) fluorescence difference gel

electrophoresis (DIGE) analysis coupled with Pro-Q Diamond staining, and demonstrated that the functional association of neurofibromin and CRMP-2 is essential for neuronal cell differentiation (7). In these studies, neurofibromin expression was suppressed using small interfering RNA (siRNA) directed against NF1, and the inhibition of neurofibromin functions caused neurite retraction via the regulation of Ras-MAPK-CDK5-GSK3/ROCK activation in differentiated PC12 cells stimulated by NGF (7). These results indicated that the neurofibromin-deficient PC12 cell is a useful model for analyzing NF1-related molecular pathology in detail.

Our previous research has examined specific genes and proteins related to phenotypic changes in neural tumors using integrated proteomic techniques such as 2D-DIGE combined with Pro-Q Diamond staining to identify phosphorylated proteins, isobaric tagging for relative and absolute quantitation (iTRAQ) (7, 8), which provides information on peptide/protein quantitative expression levels from different sources in a single experiment by liquid chromatography combined with tandem mass spectrometry (LC-MS/MS), as well as DNA array technology, utilizing the original data mining tool, MANGO (Molecular Annotation by Gene Ontology) (8). Processing the voluminous data arising from each analysis highlighted the need for a mining system for data integration. Therefore, we created the "iPEACH" (Integrated Protein Expression Analysis Chart, PCT/JP2011/58366) application to integrate information from several analysis types into a useful data file that provides comprehensive proteomic data including post-translational modification, transcriptomic data, and functional annotations from several databases, with a tool for quickly organizing, enriching, and sorting these data to reveal candidate molecules. Using iPEACH, sample data obtained from our transcriptomic and proteomic (iTRAQ and 2D-DIGE) analyses of NF1 disease model cells were integrated and stored in a database.

In this study, we constructed an iPEACH database for neurofibromin-deficient PC12 cells

compared with normal cells after NGF stimulation, and used Gene Ontology (GO) and knowledge-based network analyses targeting upregulated signals in the NF1 model cells, which lost their normal differentiation activity, to extract a novel candidate signal network for NF1-related phenotype, termed "dynein IC2-GR-CO□1" signaling. Statistical analysis of the expression or modification of these proteins in NF1-knockdown (NF1-KD) cells and subsequent biological validation by sequential analyses using siRNAs and the glucocorticoid receptor (GR) antagonist led to the successful identification of protein targets of the network most likely to be involved in the abnormal PC12 differentiation caused by neurofibromin deficiency. In addition, this network involved the alternative splicing and specific phosphorylation of cytoplasmic dynein 1 intermediate chain 2 isoform □ (dynein IC2-□) and isoform C (dynein IC2-C) via NGF stimulation in NF1-KD PC12 cells.

Here, we demonstrate that the function of neurofibromin for neurite outgrowth in PC12 cells may involve the regulation of cyclooxygenase-1 (CO□-1) via glucocorticoid receptor (GR) and dynein IC2 splicing and phosphorylation. □e also discuss the implications of a functional association between neurofibromin and CO□-1 for neuronal regulation in relation to NF1 pathogenesis. This report is the first to identify a signal network related to NF1 phenotype in a neurofibromin-deficient neural model using our new integrated proteomics strategy.

Experimental procedures

Cell culture, NGF treatment, transfection, and preparation of cell lysate

PC12 cells were cultured under 5□ CO_2 at 37□C in Dulbecco□s modified Eagle□s medium (Invitrogen)

supplemented with 10□ horse serum and 5□ fetal bovine serum. Transfection of siRNA was performed with the Neon transfection system (Invitrogen) according to the manufacturer□s protocol (1100 □, 20 ms, two times). PC12 cells were transfected with siRNA and then seeded onto collagen-coated culture dishes (Iwaki). At 2□h after transfection, PC12 cells were stimulated with 50 ng/ml 2.5S NGF (□ako) until harvest. Cells were washed twice in P□S and solubilized with lysis buffer containing 8 M urea, 2□ (w/v) CHAPS, 1 mM DTT, 10 mM sodium fluoride, 2 mM sodium orthovanadate, 1 □M okadaic acid, and 1□ (v/v) protease inhibitor mixture (Sigma). Lysates were passed through a 25-gauge syringe 20 times and centrifuged at 20,000 × *g* for 15 min at □ □C, and the protein concentrations of the supernatants were determined using Protein Assay Dye Reagent Concentrate (□io-Rad). Cellular phenotypic changes were monitored on a time-lapse microscope equipped with a CO_2 incubation chamber system (I□81, Olympus) using MetaMorph software ver. 7.5.5.0 (Molecular Devices).

RNA isolation and microarray analysis

Total RNA was extracted and purified with the RNeasy Mini Kit (Qiagen) according to the manufacturer□s instructions. Isolated RNA was assessed for quantity and quality using a NanoDrop ND1000 spectrophotometer (Thermo Scientific) and a 2100 □ioanalyzer (Agilent). Double-stranded complementary DNA (cDNA) and labeled complementary RNA (cRNA) were synthesized from the total RNA using the 3′ I□T Express Kit and hybridized to Affymetrix Rat 230 2.0 gene chips (Affymetrix). The chips were scanned with a Gene Chip Scanner 3000. The probe-level raw data and CEL files were obtained using GeneChip Operating Software. The raw expression data from CEL files was normalized by MAS5 algorism and analyzed by Subio Platform software (ver. 1.12, Subio, Japan).

2D-DIGE and image analysis

PC12 cell lysates were desalted using a 2D Clean-up kit (GE Healthcare) and dissolved in lysis buffer

containing 8 M urea, 2□ (w/v) CHAPS, and 30 mM Tris-HCl (pH 8.5). Each sample (50 □g) was minimally labeled with □00 pmol of either Cy3 or Cy5 for comparison on the same gel. To facilitate image matching and cross-gel statistical comparison, a pool of all samples was prepared and labeled with Cy2 (□00 pmol/50 □g) as an internal standard for all gels. The labeling mixture was incubated on ice in the dark for 30 min, and the reaction was terminated by addition of 10 nmol lysine. The differentially Cy3- and Cy5-labeled samples were mixed with Cy2-labeled internal standard and incubated with equal volumes of 2× sample buffer containing 8 M urea, 2□ (w/v) CHAPS, 2.□□ (v/v) Destreak Reagent (GE Healthcare), and 1□ (v/v) IPG buffer (pH 3□1 or pH □□7, GE Healthcare) for 10 min on ice. The mixed samples were supplemented with 1× sample buffer containing 8 M urea, 2□ (w/v) CHAPS, 1.2□ (v/v) Destreak Reagent, and 0.5□ (v/v) IPG buffer to reach a final volume of □50 □l and loaded into strip holders for first-dimension isoelectric focusing (IEF). IPG strips (pH 3□1 NL or pH □□7, 2□ cm, GE Healthcare) were rehydrated with the Cy-labeled samples in the dark at room temperature overnight. IEF was performed using a Multiphor II apparatus (GE Healthcare) under the following conditions□held at 100 □ for 2 h, held at 500 □ for 2 h, ramped to 1,000 □ in 5 h, ramped to 8,000 □ in 3 h, and held at 8,000 □ for □h for pH 3□1 NL strips□held at 100 □ for 2 h, held at 500 □ for □h, ramped to 1,000 □ in 5 h, ramped to 8,000 □ in 3 h, and held at 8,000 □ for □5 h for pH □□7 strips. Strips were equilibrated in solution containing 2□ (w/v) SDS, 50 mM Tris-HCl (pH 8.8), 6 M urea, 30□ (v/v) glycerol, 0.002□ (w/v) bromophenol blue, and 1 mM DTT for 20 min and then in the same buffer additionally containing 1 mM iodoacetamide for 20 min. The equilibrated strips were then transferred onto 10□ gels (2□× 20 cm) for second-dimension electrophoresis using the Ettan DALTsix system (GE Healthcare). SDS-PAGE was run at 10 mA/gel for 1 h and then 12 mA/gel at 30□C until the bromophenol dye front reached the gel end. Images of protein spots on the gels were scanned with a